Comparison of the lipid acyl chain dynamics between small and large unilamellar vesicles

Leslie S. Lepore, Jeffrey F. Ellena, and David S. Cafiso
Department of Chemistry and Biophysics Program, University of Virginia, Charlottesville, Virginia 22901

ABSTRACT ^{13}C NMR spin-lattice relaxation (T_1) rates and ^{13}C–^1H nuclear Overhauser effects (NOEs) were measured in an identical fashion in two lipid preparations having dramatically different curvatures. The T_1 times that were obtained at four magnetic field strengths were fit along with the NOEs to simple models for lipid molecular dynamics. The results indicate that phospholipid chain ordering and dynamics are virtually identical in small and large unilamellar vesicles at the time scales sampled by these ^{13}C-NMR studies. The order parameters and reorientational correlation times that characterize the amplitudes and rates of internal acyl chain motions were equal within experimental error for the methylene segments in the middle of the chains. The only significant differences in order parameters and correlation times between the two vesicle types were small and appeared at the ends of the acyl chains. At the carbonyl end the order was slightly higher in small vesicles than large vesicles, and at the methyl end the order was slightly lower for small vesicles. This indicates that in the more planar systems the acyl chains exhibit a slightly flatter order profile than in more highly curved membranes. The use of the same experimental approach in both small and large vesicle systems provided a more reliable and accurate assessment of the effect of curvature on molecular order than has been previously obtained.

INTRODUCTION

Model membrane systems are extremely important and widely utilized tools for the study of biological membranes and membrane-associated proteins. Not surprisingly, a wide range of procedures to prepare model bilayer membranes is available, and the morphology of these systems is quite varied. One of the more popular techniques employed was first described over two decades ago and involved the ultrasonic irradiation of multilamellar lipid dispersions to produce small vesicles (Huang, 1969). The vesicles that are formed by this technique are well sealed, homogeneous, unilamellar, and appear to be a minimal size for vesicles ($\approx$150 Å). In fact, the curvature of the membrane in these vesicles is high enough so that the lipids are packed differently on the internal and external surfaces (Huang and Mason, 1978).

The relationship between lipid organization in small vesicles (such as those produced by sonication) and lipids in large vesicles (or multilamellar dispersions) is a question that frequently confronts experimentalists who use model membranes. As a result, there is an interest in understanding to what extent these small structures are different in their lipid organization from other model and biological membrane systems. From a more fundamental perspective, numerous studies have shown that biological membrane function is dependent on membrane phospholipid structure and dynamics (Gennis, 1989). Because highly curved membranes are found in some naturally occurring membrane systems, such as the inner mitochondrial membrane or the photoreceptor disk edges, there is also an interest in understanding how membrane curvature affects the properties of the bilayer lipid.

A number of experimental studies, based primarily upon NMR, have examined the effect of membrane curvature on the rates and amplitudes of motions in phospholipid acyl chains. Unfortunately, the conclusions reached have not been consistent. Several studies have concluded that the order parameters that describe the restriction of fast motions in the lipid acyl chains are two to three times smaller in small vesicles compared with large unilamellar systems (Bocian and Chan, 1978, and references therein; Fuson and Prestegard, 1982; Parmer et al., 1984), whereas other experimental studies suggest that the fast motional order parameter of vesicles is the same or only slightly smaller than multilamellar bilayers (Stockton et al., 1976; Bloom et al., 1978; Kintanar et al., 1986; Korstanje et al., 1989). There appear to be at least two sources for the discrepancies that are seen in the literature. First, most of the NMR work described above utilized lineshape analyses and spin relaxation measurements. The interpretation of these data in terms of molecular order often relies on estimates of molecular diffusion and vesicle sizes, two quantities that are difficult to determine precisely. Second, to make the comparison with bilayers that lack curvature, the order parameters obtained for small

Address correspondence to Dr. Cafiso.

0006-3495/92/03/767/09 $2.00

vesicles have typically been compared with order parameters obtained using a completely different approach in unsonicated multilamellar membranes (for example, wideline ^2H NMR).

In the present study, we describe a more direct approach that involves making the same spin-lattice relaxation (T_1) and nuclear Overhauser effect (NOE) measurements in two vesicle populations having average diameters of 350 and 950 Å. ^{13}C T_1 measurements were made at four frequencies between 15 and 125 MHz, and ^{13}C NOE measurements were made at 15 MHz. The data were analyzed in terms of a model that has received considerable previous support and yields quantitative information on molecular ordering and dynamics of the phospholipid (Brown, 1984; Pastor et al., 1988). The results provide strong evidence that bilayer curvature has little if any effect on the amplitudes and rates of those motions that contribute to ^{13}C T_1 and NOE. These are motions with rates between 10^{12} and 5×10^7 rad/s.

MATERIALS AND METHODS

Preparation and characterization of phospholipid vesicles

Palmitoyloleoylphosphatidylcholine (POPC) was obtained from Avanti Polar Lipids, Inc. (Birmingham, AL) and the $CHCl_3$ solution was dried by rotary evaporation followed by high vacuum overnight. Preparation of the lipid vesicle suspensions began by hydrating the lipid with 25 mM sodium phosphate, pH 7.0. Small lipid vesicles were formed by ultrasonically irradiating the lipid mixture using a procedure described previously (Castle and Hubbell, 1976). Large vesicles were prepared by freeze thawing the lipid–buffer mixture five times in liquid nitrogen, followed by extrusion 10 times through an 800-Å polycarbonate filter using a commercially available unit (Lipex Biomembranes Inc., Vancouver, BC). Electron microscopy was carried out on these vesicle suspensions to determine vesicle sizes as described previously (Castle and Hubbell, 1976). Briefly, this procedure involved fixation of the lipid vesicles in 0.5% osmium tetroxide followed by deposition of the vesicles onto formvar- and carbon-coated 200-mesh copper grids with 1% uranyl acetate used as the negative stain. The sizes and distribution of sizes for these vesicle suspensions were 350 ± 100 Å for the sonicated vesicles and 947 ± 270 Å.

NMR spectroscopy

^{13}C NMR spectra were recorded at four frequencies: 15, 75, 90, and 125 MHz with NMR spectrometers (FX60Q [JEOL USA Inc., Peabody, MA], GN300 [General Electric Co., Wilmington, MA], NT360 [Nicolet Instrument Corp., Madison, WI], and Omega 500 [General Electric Co.], respectively). Proton decoupling schemes included noise modulation (Fukushima and Roeder, 1981), MLEV-64 (Levitt et al., 1982), 90,180 square wave (Grutzner and Santini, 1975), and Waltz-16 (Shaka et al., 1983), respectively. Protons were decoupled throughout the T_1 experiments. All the spectrometers had temperature control accessories, and the sample temperatures were measured with a thermocouple that was inserted into the sample in the magnets. The spectrometer temperature controllers were adjusted so that the temperature of the sample was 32°C. T_1 times were measured by the fast inversion recovery method, and T_1 values were obtained by a three-parameter fit of the peak amplitudes (Craik and Levy, 1984). ^{13}C NOEs were obtained by measuring the ratio of peak amplitudes of spectra recorded with ^1H decoupling throughout the experiment and spectra with ^1H decoupling only during the acquisition. When adjusting delay times in NOE experiments, care was taken to make sure that carbon magnetization returned to equilibrium after each acquisition and that sufficient time was allowed for complete NOE buildup (Canet, 1976). Recycle times for the NOE experiment were set at 7–10 times the longest T_1 value at 60 MHz.

Analysis of NMR data

The relaxation behavior of the ^{13}C nucleus is dominated by the interaction of the C nucleus with its directly bonded proton(s); as a result, the spin–spin relaxation rate and NOE for ^{13}C are determined by the motions of the C–H bond vector with respect to the applied magnetic field. In the present analysis, two slightly different spectral density functions are used to analyze the ^{13}C T_1 rates and NOEs in the vesicle systems. These spectral density functions, $J(\omega)$, describe the power spectrum for the molecular motions. The model for molecular motions that will be used here was originally introduced by Chan and co-workers (Bocian and Chan, 1978) and further developed by Brown (1982, 1984) and by Szabo and co-workers (Pastor et al., 1988). Lipids in a bilayer can undergo several motions that occur at frequencies in excess of the angular Larmor frequency (ω) and are due to internal rotations in the acyl chains (i.e., rotations about bonds, torsions, librations). Rotation of the phospholipids about their long axis also appears to occur at frequencies similar to those of the internal rotations. Finally, a much slower motion can occur that is due to the angular movement of the phospholipid long axis relative to the bilayer normal or director. This movement is commonly referred to as chain tilting or wobbling and occurs at a frequency that is less than or similar to the Larmor frequencies used here. Motions due to the overall tumbling of the vesicle or the lateral diffusion of the phospholipid are much slower and do not significantly contribute to the ^{13}C T_1 and ^1H–^{13}C NOE at the Larmor frequencies used here.

The simplest spectral density function that has been shown to fit adequately the ^{13}C T_1 data for phospholipid vesicles collected over the frequency range used here is:

$$J(\omega) = \left(\frac{S_j^2\tau_T}{1 + (\omega\tau_T)^2}\right) + (1 - S_j^2)\tau_j, \quad (1)$$

where τ_j is the correlation time for reorientation due to internal motions and axial rotations (henceforth referred to as fast motions), S_j is the order parameter for fast motions, τ_T is the correlation time for chain tilting, and ω is the Larmor frequency. This spectral density function resembles one used by Lipari and Szabo (1982) in their model-free approach. A similar but physically more reasonable spectral density function is given by:

$$J(\omega) = \left[\frac{(1 - S_T^2)S_j^2\tau_T}{1 + (\omega\tau_T)^2}\right] + (1 - S_j^2)\tau_j, \quad (2)$$

where all the parameters are the same as for Eq. 1, except that an order parameter, S_T, has been added to describe the amplitude of the phospholipid tilt. The derivation of the above spectral densities assumes that fast and tilt motions are independent and axially symmetric. The order parameter S_j is $0.5(3\cos\Theta - 1)$, where Θ is the time-averaged angle between the C–H internuclear vector and the symmetry axis for motional averaging.

While the above spectral densities do not result from a rigorous description of motion in phospholipid bilayers, their ability to fit T_1

data over a wide frequency range indicates that they provide a reasonable description of lipid molecular order and dynamics in a bilayer. Therefore, they are appropriate quantitative tools for the purpose of this study, which is to examine the effect of phospholipid vesicle curvature on lipid order and dynamics. The spectral densities given in Eqs. 1 and 2 above do not take into account fluctuations in the orientation of the membrane order director. While some models for bilayer T_1 have included these motions, recent work suggests that they do not make a significant contribution to T_1 or NOE measurements at the Larmor frequencies used here (Pastor et al., 1988; Rommel et al., 1988; Mayer et al., 1990).

As described above, both the ^{13}C spin-lattice relaxation rate (T_1^{-1}) and the NOE can be related to magnitude and frequencies of the molecular motions, as given by Doddrell et al. (1972):

$$\frac{1}{T_1} = \frac{N}{20}\left(\frac{\gamma_H\gamma_C h}{r^3}\right)^2 [J(\omega_H - \omega_C) + 3J(\omega_C) + 6J(\omega_H + \omega_C)] \quad (3)$$

$$NOE = 1 + \frac{\gamma_H}{\gamma_C}\left[\frac{6J(\omega_H + \omega_C) - J(\omega_H - \omega_C)}{J(\omega_H - \omega_C) + 3J(\omega_C) + 6J(\omega_H + \omega_C)}\right], \quad (4)$$

where N is the number of directly bonded hydrogens, γ_H and γ_C are the hydrogen and carbon magnetogyric ratios, h is Planck's constant, r is the C—H bond distance, and $J(\omega)$ are the spectral densities in terms of the angular resonant frequencies for ^{13}C (ω_C) and ^1H (ω_H). The value for $(\gamma_H\gamma_C h/r^3)$ is $1.3652 \times 10^5\ s^{-1}$ (Soderman, 1986).

Determining the lipid dynamics from the T_1 and NOE data

The experimental T_1 and NOE data were analyzed in terms of the two spectral density functions listed above in Eqs. 1 and 2. To obtain a fit of the relaxation data to the lipid molecular dynamics, the error function shown below, Eq. 5, was minimized for the two correlation times and the order parameter for internal motion. In the analysis made here, the correlation time for the molecular tilting, τ_T, was assumed to have an identical value for all positions along the acyl chain.

$$\text{Error} = \sum_{\omega}\left(\frac{NOE_{calc} - NOE_{exp}}{NOE_{exp}}\right)^2 + \left(\frac{T_{1calc} - T_{1exp}}{T_{1exp}}\right)^2 \quad (5)$$

Two procedures were used to fit the data. In the first, the fitting was aided by the use of a downhill simplex routine (see Nelder and Mead, 1986) to determine the values of τ_j, S_j that yield a minimum in the error function, Eq. 5. This was done for a range of physically reasonable values of τ_T that were applied to each C position. In a second, less elegant, procedure, a three-dimensional grid that included all reasonable values of τ_j, S_j, and τ_T was searched to determine those values that produced a minimum in the error function. Again the value of τ_T was held constant for each carbon position along the acyl chain. In the analyses presented below, the fits obtained by the simplex routine were in very close agreement with the fits obtained by the more straightforward "grid searching" routine. For the spectral density given in Eq. 2, the amount of data that was collected did not permit a simultaneous fit of the four parameters S_T, S_j, τ_T, and τ_j to a high degree of precision. As a result, the fits were carried out at several values of the tilt order parameter, S_T, between 0.52 and 0.68. In this analysis S_T was assumed to be the same for large and small unilamellar vesicles. This appears to be a reasonable assumption based on previous fluorescence and EPR data showing that S_T differs by <20% between these two vesicle types (Stubbs et al., 1981; Kinosita and Ikegami, 1984; Korstanje et al., 1989).

RESULTS

Shown in Fig. 1 are the 15- and 125-MHz ^{13}C spectra of POPC along with the ^{13}C resonance assignments (resonance assignments are those of Brainard and Cordes, 1981). Although the 15-MHz spectrum is more crowded than the 125-MHz spectrum, the 15-MHz spectrum provides resolution that is sufficient for both T_1 and NOE measurements of most of the assigned resonances. In two cases (the $C_{\omega-2}$ and $\underline{C}H_2$—C=C positions), resonance overlap precluded separate measurements for the individual carbons in the overlapped peaks; however, these atoms have very similar locations in the POPC molecule and the bilayer, and therefore measurement of an average T_1 and NOE is appropriate. The T_1 values obtained at four frequencies and NOE values obtained at 15 MHz for the 350- and 950-Å vesicles are shown in Table 1. The relaxation data for the two vesicle sizes is close, and in most cases the differences are less than the experimental error (10%). The largest differences that show up between these two data sets appear at the ends of the lipid acyl chains. For example, the relaxation times for the methylenes near the carbonyl end of the acyl chains (the C_2 and C_3 positions) are higher for the 950-Å than for the 350-Å vesicles, but the differences are not large and are typically <25%. The

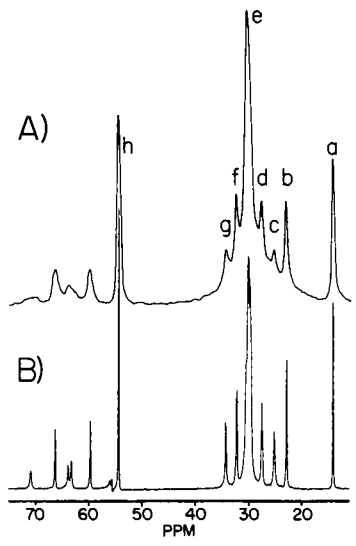

FIGURE 1 Proton-decoupled ^{13}C spectra of small sonicated POPC vesicles recorded at (*A*) 15 and (*B*) 125 MHz. Several of the assignments for the carbon spectra are (*a*) —CH_3; (*b*) —$\underline{C}H_2CH_3$; (*c*) —OCO—C—$\underline{C}H_2$; (*d*) —$\underline{C}H_2$—C=; (*e*) —$(CH_2)_n$—; (*f*) —$\underline{C}H_2$—C—CH_3; (*g*) —OCO—$\underline{C}H_2$; and (*h*) —$N^+(CH_3)_3$. Resonances that are shown downfield from the headgroup nitrogen are in the headgroup and glycerol backbone. The peaks seen at ~56 ppm are due to vinyl resonances that are folded in.

TABLE 1 ^{13}C T_1s and ^1H-^{13}C NOEs

Carbon position	125 MHz		90 MHz		75 MHz		15 MHz		NOE (15 MHz)	
	350 Å	950 Å	350 Å	950 Å	350 Å	950 Å	350 Å	950 Å	350 Å	950 Å
—$\underline{CH_2}CH_3$	2.130	2.040	1.523	1.534	1.467	1.366	1.086	0.823	2.82	2.95
—$\underline{CH_2}C$—CH_3 (sn-2)	1.486	1.241	1.081	0.903	0.895	0.770	0.559	0.469	2.66	2.84
—$\underline{CH_2}$C-CH_3 (sn-1)	1.513	1.241	1.061	0.903	0.878	0.770	0.559	0.469	2.66	2.84
—$(\underline{CH_2})_n$—	0.773	0.786	0.580	0.603	0.502	0.523	0.329	0.324	2.62	2.79
$\underline{CH_2}$—C=C— (a)	0.648	0.635	0.505	0.555	0.418	0.463	0.300	0.286	2.69	2.60
$\underline{CH_2}$—C=C— (b)	0.661	0.635	0.502	0.555	0.426	0.463	0.300	0.286	2.69	2.60
—CO—C—$\underline{CH_2}$—	0.482	0.497	0.410	0.494	0.314	0.384	0.226	0.266	2.70	2.35
—CO$\underline{CH_2}$—	0.375	0.434	0.274	0.437	0.235	0.337	0.172	0.223	2.34	2.19

Two sets of spin-lattice relaxation times for each megahertz value (T_1, in seconds) and two sets of nuclear Overhauser effects (NOEs) for 15 MHz are given in this table and represent values obtained in small (350 Å) and large (950 Å) unilamellar vesicles. The relaxation times and NOEs were obtained as described in the text. Separate carbon resonances for the —$\underline{CH_2}CH_2CH_3$ and $\underline{CH_2}$—C=C— positions could not be resolved for the 950 Å vesicles or for the sonicated vesicles at 15 MHz, and these separate entries actually represent one measurement. Two allylic positions, listed (*a*) and (*b*), are resolved, but have not been assigned.

T_1s for the methylenes adjacent to the methyl end of the acyl chains (the $C_{\omega-1}$ and $C_{\omega-2}$ positions) are higher for the 350-Å vesicles; however, these difference are again $<20\%$.

As described above, the two spectral density functions given by Eqs. 1 and 2 were used to fit the data. When Eq. 1 was used to fit the relaxation data, values for the slow correlation time (τ_T) of 1.5 and 1.9 ns were obtained for the small (350 Å) and large (950 Å) vesicles, respectively. Four fits were performed using the more complex spectral density described by Eq. 2 at S_T values ranging from 0.52 to 0.68. This represents the expected range in S_T values based on previous work (Peterson and Chan, 1977; Oldfield et al., 1978; Taylor et al., 1982; Meier et al., 1986; Pastor et al., 1988; Mayer et al., 1990). For $0.52 < S_T < 0.62$, fitting the data with Eq. 2 yielded a value for τ_T of 1.9 ns for both the 350- and 950-Å vesicles. When S_T was set to 0.68, the fit yielded a slightly different value for τ_T of 1.8 ns for both 350- and 950-Å vesicles. Shown in Fig. 2 are the values of order parameter, S_j, that were obtained from fits of the data to Eq. 1 and 2. Similar values of S_j are obtained using the two spectral density functions, and all but the lowest values of S_T produce values of S_j that are within $\sim 25\%$ when these two functions are compared. Fig. 3 shows the values of τ_j that were obtained from the same fits. Nearly identical values of τ_f are obtained using the two spectral density functions defined by Eqs. 1 and 2. As the value of S_T is varied from 0.52 to 0.68 in Eq. 2, the value of S_j that fits the data best is increased by 20%, and the best value for τ_j changes by $<10\%$.

Fig. 2 clearly reveals the expected dependence of S_j on segment position. This segment dependence of S_j decreases from the carbonyl to the methyl end of the acyl chain, and is also known as the order profile or order

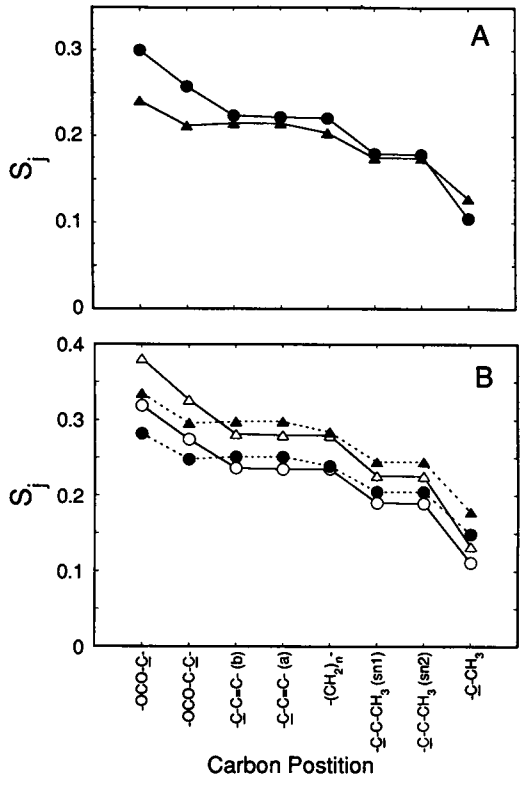

FIGURE 2 The order parameter for internal chain motions, S_j, was determined from the frequency-dependent T_1 and NOE data and is plotted as a function of segment position. (A) The results of an analysis using the spectral density function defined in Eq. 1 for 350- (●) and 950-Å (▲) diam unilamellar vesicles. Lines connecting the points are shown to clarify the trends in S_j. (B) The results of an analysis using the spectral density defined in Eq. 2. The results for 350-Å-diam vesicles are shown using values of the tilt order parameter, S_T, of 0.52 (○) and 0.68 (△). For the 950-Å vesicles, the results of using S_T values of 0.52 (●) and 0.68 (▲) are also shown. The error in the order parameter, S_j, is $\sim 10\%$.

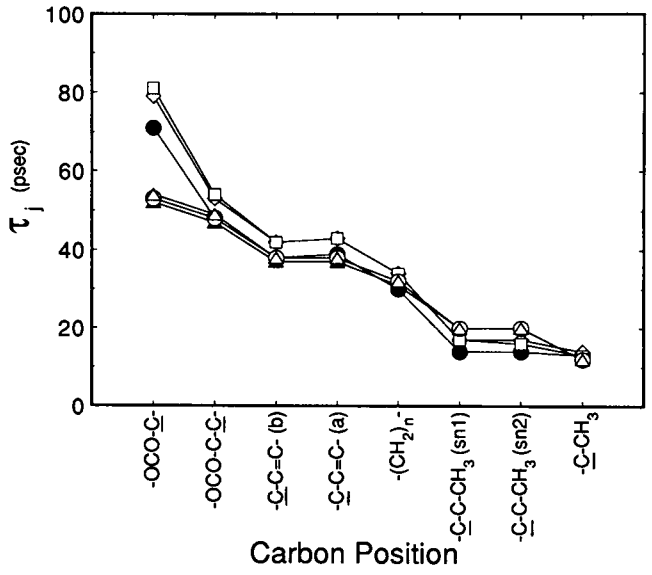

FIGURE 3 The correlation time, τ_j, representing fast internal chain motions (such as segmental motions) is plotted as a function of the segment position. Neither the spectral density function used in the analysis nor the vesicle size had much effect on the values of τ_j for a particular segment (●) 350- and (▲) 950-Å-diam vesicles fit to the spectral density represented by Eq. 1. 350-Å vesicles fit to Eq. 2 with $S_T = 0.52$ (◇) or 0.68 (□), and 950-Å vesicles fit to Eq. 2 with $S_T = 0.52$ (○) or 0.68 (△).

gradient. This dependence is similar for the 350- and 950-Å vesicles. There are, however, small but significant differences that show up regardless of the spectral density function that is used to obtain the values of S_j. The order profile for the large vesicles is flatter than that for the small vesicles, and the greatest differences between the two vesicle sizes occur at each end of the acyl chains. These results indicate that the gradient in the order parameter is slightly steeper for the small vesicles, being more ordered at the headgroup and less ordered at the methyl end of the acyl chain compared with the large vesicles. The differences in S_j are 25% at the $C_{\omega-1}$ position and 20% at the C_2 position. As seen in Fig. 3, the dependence of τ_j on segment position is also very similar for 350- and 950-Å vesicles. The largest difference occurs at the C_2 position, where there is a 30% difference between the two vesicle types; differences in τ_j are considerably smaller for the other positions. For most of the acyl chain carbon positions examined here, size alters S_j and τ_j by $<20\%$ and has at most 30% effect on the ends of the chains. These findings provide strong evidence that membrane curvature has little effect on the rates and amplitudes of the fast lipid acyl chain internal motion.

DISCUSSION

In the present work, the effect of membrane bilayer curvature on the acyl chain methylene segmental order and dynamics was estimated by measuring ^{13}C T_1 times and NOEs for vesicles of two different sizes. By analyzing the data in terms of relatively simple but physically reasonable models, little or no difference is found between the order and dynamics of lipids in small and large vesicles (see below for a discussion of these models). The order parameters and correlation times of methylene segments in the middle of the acyl chains are equal within experimental error, and the only significant differences that are revealed are small. These differences occur at each end of the acyl chain, such that the average lipid in a small vesicle exhibits a slightly larger order gradient than lipids in less curved bilayers. The order gradient in the smaller vesicles is also more uniform; that is, the characteristic plateau normally seen in the planar systems toward the headgroup is not as apparent. A more uniform decrease in order from the polar to the methyl end of amphiphilic molecules is also seen in micelles (Karaborni and O'Connell, 1990, and references therein) and inverted hexagonal (H_{II}) phases (Lafleur et al., 1990). Comparing the geometries of the different phases, the molecular packing in the outer leaflet of small vesicles should be intermediate between the packing in a planar bilayer and a spherical micelle. Similarly, lipids in the inner leaflet should be intermediate in their packing between that in a planar bilayer and an H_{II} phase. The observed difference between the order gradients of large and small vesicles is qualitatively consistent with this description of the chain packing in small vesicles; however, it should be emphasized that the order parameters between large and small vesicles are very similar in absolute terms, and the amount of "nonbilayer packing character" in the small vesicles is minor.

To gain an appreciation for the difference in curvature between the two vesicle populations examined here, the number of molecules in the outer and inner leaflets of the bilayer was compared. To make this comparison, the population was subdivided according to size, outside/inside ratios were calculated for each subpopulation, and the subpopulations were finally weighted according to the number of lipids per vesicle (Bloom et al., 1978). Based on this statistical treatment, along with a bilayer thickness of 43 Å (Caffrey and Feigenson, 1981) and the POPC area at the membrane surface of 75.6 $Å^2$ (Lis et al., 1982), values of 1.74 and 1.21 were obtained for the outside/inside ratios of the small and large vesicles, respectively. These ratios indicate that the large vesicles

have a curvature that is much closer to that of a planar bilayer (ratio = 1.0) than to the small vesicle curvature. Thus, if a significant difference in segmental order and/or dynamics existed between small vesicles and planar bilayers, that difference should have been revealed by examining the two vesicle populations studied here.

In the analysis made here using Eq. 2, it is assumed that S_T is approximately the same in large and small unilamellar vesicles. However, it is conceivable that S_T and S_j both differ in small and large unilamellar vesicles by amounts that allow the spectral density function to remain unchanged between the two vesicle types. In this case, the analysis would fail to reveal the effects of curvature. This is not a likely possibility for at least two reasons. First, fluorescence and EPR data provide no indication that the value of S_T is dramatically different in small and large unilamellar vesicles (Stubbs et al., 1981; Kinosita and Ikegami, 1984; Korstanje et al., 1989). In fact, the value of S_T is different by $<20\%$ when small vesicles are compared with planar bilayer systems. These techniques are sensitive to motions on the 0.1-GHz time scale and should include the tilting motion studied here (here, $1/\tau_T$ is ~ 0.5 GHz). Second, there are a limited number of fortuitous combinations of S_T and S_j that will yield no difference between the two systems.

Compared with previous ^{13}C relaxation studies, the order parameters and correlation times that are obtained here for the small POPC vesicles are similar to values that have been obtained for small sonicated dipalmitoylphosphatidylcholine vesicles in the liquid crystalline phase (Brown, 1984; Pastor et al., 1988). However, previous NMR studies aimed at providing a measure of the effect of bilayer curvature on phospholipid order have yielded quite different and inconsistent conclusions. Several studies found no dependence of order on bilayer curvature (Finer et al., 1972; Horwitz et al., 1973; Finer, 1974; Stockton et al., 1976; Bloom et al., 1978), whereas other reports (Sheetz and Chan, 1972; Seiter and Chan, 1973; Lichtenberg et al., 1975; Bocian and Chan, 1978; Fuson and Prestegard, 1983b; Parmar et al., 1984) claimed a substantial decrease in segmental order in highly curved bilayers (i.e., sonicated vesicles) compared with bilayers with little curvature (i.e., multilamellar phospholipid dispersions). One problem that contributes to the uncertainty of this previous work is that the order in highly curved and planar bilayers was measured using fundamentally different experimental approaches. In multilamellar systems that have a low curvature, a direct measurement of order can be obtained by measuring the residual quadrupolar splitting of a deuterium-labeled lipid; the splitting is then interpreted in a straightforward manner in terms of the order parameter (Seelig, 1977). Unfortunately this measurement is not possible for small vesicles because the residual quadrupolar splitting is dominated by vesicle tumbling rather than by phospholipid order. To obtain a measure of phospholipid order in vesicles, relaxation or linewidth measurements have typically been utilized. The approach taken here allows for a more direct and reliable estimate of the effect of membrane curvature on lipid ordering because the same measurement has been carried out for bilayers with different degrees of curvature.

The use of different NMR experiments to determine curvature effects may yield different order parameters even if the lipids behave identically. When comparing order parameters obtained from different types of measurements, the range of motional frequencies that may contribute to the observed order must be considered. For example, the low frequency cutoff for motions contributing to measurements usually made in vesicles is close to 1 MHz for ^1H and ^2H linewidth measurements, and ~ 10 MHz for ^{13}C T_1 measurements. This is significantly higher than for measurements of the residual quadrupolar splitting in multilamellar dispersions, where the cut-off frequency is ~ 170 kHz. Thus, differences in the estimates for the segmental order may simply reflect the different time scales that are being sampled.

Most previous NMR studies of molecular order in small vesicles have involved linewidth measurements, and these measurements likely yield values for S that have a considerable degree of uncertainty. In these experiments, it is assumed that the major part of the linewidth can be described by:

$$v = KS^2\tau_v, \tag{6}$$

where v is the linewidth at half maximum, K is a constant that depends on the nucleus observed, S is the order parameter, and τ_v is the vesicle correlation time (Bocian and Chan, 1978). τ_v is defined by:

$$\frac{1}{\tau_v} = \frac{1}{\tau_R} + \frac{1}{\tau_D} = \frac{3kT}{4\pi\eta R^3} + \frac{6D}{R^2}, \tag{7}$$

where τ_R is the correlation time for vesicle rotation, τ_D is the correlation time for molecular motion due to diffusion in the vesicle, k is Boltzman's constant, T is the absolute temperature, η is the solvent viscosity, R is the vesicle radius, and D is the lateral diffusion constant for phospholipid motion in the vesicle. Many measurements of lateral diffusion in the liquid crystalline phase have been made; the values, which are in general independent of phospholipid type and acyl chain length, range from 1×10^{-8} to 2×10^{-7} cm^2 s^{-1} (Wade, 1985). Taking the temperature to be 32°C, using the mass-based average radius for the small vesicles of 196-Å, and assuming a diffusion constant of 8×10^{-7} cm^2 s^{-1}, it can

be shown that $\tau_R/\tau_D = 1.4$. Thus, both τ_R and τ_D make substantial contributions to τ_v. Because τ_R and τ_D are dependent on R^3 and R^2, respectively, small uncertainties in R become important in the determination of τ_v. Combined with the substantial uncertainty in D, τ_v (and therefore S) must have a considerable level of uncertainty.

Fuson and Prestegard (1983*b*) took an approach different from those described above and performed proton-coupled ^{13}C spin relaxation experiments on small vesicles and multibilayers containing labeled acyl chains. They measured auto- and crosscorrelation spectral densities and fit their data to various motional models. In their work on small vesicles containing a ^{13}C-labeled fatty acid, they calculated an acyl chain order parameter that was approximately half of that of multibilayers. Unfortunately, the method used to calculate the molecular order was not shown. In a subsequent study of vesicles and multibilayers, in which the ^{13}C chain was incorporated into the phospholipid, no comparison of order in small vesicles and low curvature bilayers was made (Fuson and Prestegard, 1983*a*). Because of the limited information on the extraction of order parameters from the data of Fuson and Prestegard, it is difficult to assess the uncertainty in their results.

A number of techniques other than NMR have been used to estimate the effect of bilayer curvature on molecular ordering and dynamics. These techniques include fluorescence (Stubbs et al., 1981; Kinosita and Ikegami, 1984) and EPR spectroscopy (Korstanje et al., 1989). The molecular order of diphenylhexatriene (DPH) in dipalmitoylphosphatidylcholine was obtained for sonicated vesicles (Kinosita and Ikegami, 1984) and multilamellar dispersions (Stubbs et al., 1981). At 51°C, these measurements yielded order parameters for multilamellar dispersions and sonicated vesicles of 0.39 and 0.32, respectively. Order parameters and molecular reorientational diffusion coefficients were also obtained for the spin-labeled sterol, 3-doxyl-5a-cholestane (CSL), in multilamellar dispersions and sonicated vesicles. At 35°C, order parameters for CSL in a multilamellar dispersion and sonicated vesicles of POPC were 0.55 and 0.46, respectively, and no difference in the reorientational rate of this label was seen between the multilamellar and sonicated preparations. These results are representative of those obtained for different phosphatidylcholines in the liquid crystalline phase over a wide temperature range. In another interesting study carried out by Kintanar et al. (1986), order parameters were obtained for ^2H-labeled DPH in multilamellar DMPC and DMPC–cholesterol mixtures by measuring quadrupolar splittings. They compared their ^2H NMR order parameters with fluorescence order information on sonicated membranes having the same lipid compositions. They found that order parameters for the sonicated vesicles were at most ~30% lower than for multilamellar dispersions.

Taken together, these EPR and fluorescence studies suggest that molecular order in sonicated vesicles is slightly lower than in multilamellar dispersions, and this result appears to be in general agreement with the data presented here. However, when comparing order measurements made with EPR and fluorescence techniques, the low frequency cutoff for motions contributing to disorder must be considered. For fluorescence and EPR spectroscopy, this cutoff frequency is considerably higher than for ^{13}C NMR and is ~0.1 GHz. In addition, it should be noted that DPH and CSL are relatively rigid; therefore, all parts of these molecules have the same order. Due to many differences and approximations, a detailed interpretation of the relatively small differences ($\leq$40%) among studies discussed above is not warranted.

Models for molecular dynamics play a critical role in the analysis of NMR relaxation data; as a result, a final comment about the choice of the models used here seems appropriate. As indicated above, nuclear spin relaxation data can be interpreted in terms of more complex motional models than those used here (see, for example, Pastor et al., 1988; Rommel et al., 1988). However, the use of these models requires molecular dynamics simulations and/or a wider range of experimental data than was obtained here. When spin relaxation data are interpreted in conjunction with molecular dynamics simulations, several processes are found to occur on a time scale near 10^{-11} s (Pastor et al., 1988). These processes include bond librations, isomerizations, and molecular rotation about the long axis of the lipid. As a result, the values found here for τ_j (which are on this time scale) are likely averages due to some or all of these motions. Nonetheless, this simplification does not appear to affect the rates and amplitudes for motion that are obtained. The values reported here for the slower correlation time, τ_T, are very similar to those obtained in studies in which more complex motional models are used (Pastor et al., 1988; Mayer et al., 1990, and references therein). With the exception of the allylic position, the product of S_T and the values of S_j (see Fig. 2) are also close to the order parameters obtained in multilamellar dispersions using deuterium NMR (S_{CD}). This close agreement of the order parameters and rates of motion obtained here with those found using more detailed models provides strong justification for the use of the simpler model.

As mentioned above, the order parameters obtained here for the allylic position do not agree with those obtained using other methods. For example, deuterium NMR measurements on POPC yield order parameters for the allylic positions that are different from each

other and smaller than the order parameters of the adjacent methylenes (Seelig and Waespe-Sarcevic, 1978). Similar results are also obtained for the vinyl positions. When inserted into current relaxation models, these order parameters predict T_1 rates for the allylic segments, which should be different from each other and lower than the relaxation rates of the other acyl chain methylenes. However, the T_1^{-1} values of the allylic positions obtained here are close to each other and comparable to those of the adjacent methylenes. Similar observations have been made in other relaxation studies (Rajamoorthi and Brown, 1991). These inconsistencies suggest that the current models for lipid chain motion are inappropriate for the motion of the allylic or vinyl segments.

In conclusion, identical T_1 and NOE measurements on two membrane vesicle populations with different degrees of curvature were made. Using a formalism that has received considerable previous support, this NMR data was used to obtain molecular ordering and dynamics for preparations of large and small vesicles. These results indicate that membrane curvatures normally encountered have little or no effect on phospholipid acyl chain order and dynamics when considering motions with rates between 10^{12} and 5×10^7 rad/s. Similar results are consistently obtained with other techniques (fluorescence and EPR spectroscopy), and this general conclusion (that order and dynamics are only weakly dependent on curvature) is consistent among studies in which the same experimental measurements have been made on bilayers with different degrees of curvature. It should be noted that these studies do not exclude the possibility of differences in the behavior of these systems at time scales that are much slower than those examined here.

We thank Frances Stephenson and Thomas Thompson for assisting us with and allowing us access to the JEOL FX60Q NMR spectrometer.

This work was supported by a grant from the National Science Foundation (BNS 8908692), and a grant from the Jeffress Trust (J-156).

Received for publication 16 July 1991 and in final form 15 October 1991.

REFERENCES

Bloom, M., E. E. Burnell, A. L. MacKay, C. P. Nichol, M. I. Valic, and G. Weeks. 1978. Fatty acyl chain order in lecithin model membranes determined from proton magnetic resonance. *Biochemistry.* 17:5750–5762.

Bocian, D. F., and S. I. Chan. 1978. NMR studies of membrane structure and dynamics. *Annu. Rev. Phys. Chem.* 29:307–335.

Brainard, J. R., and E. H. Cordes. 1981. Carbon-13 nuclear magnetic resonance studies of cholesterol–egg yolk phosphatidylcholine vesicles. *Biochemistry.* 20:4607–4617.

Brown, M. F. 1982. Theory of spin-lattice relaxation in lipid bilayers and biological membranes. ^2H and ^{14}N quadrupolar relaxation. *J. Chem. Phys.* 77:1576–1599.

Brown, M. F. 1984. Theory of spin-lattice relaxation in lipid bilayers and biological membranes. Dipolar relaxation. *J. Chem. Phys.* 80:2808–2831.

Caffrey, M., and G. W. Feigenson. 1981. Fluorescence quenching in model membranes. 3. Relationship between calcium adenosine triphosphate enzyme activity and the affinity of the protein for phosphatidylcholines with different acyl chain characteristics. *Biochemistry.* 20:1949–1961.

Canet, D. 1976. Systematic errors due to improper waiting times in heteronuclear Overhauser effect measurements by the gated decoupling technique. *J. Magn. Reson.* 23:361–364.

Castle, J. D., and W. L. Hubbell. 1976. Estimation of membrane surface potential and charge density from the phase equilibrium of a paramagnetic amphiphile. *Biochemistry* 22:4818–4831.

Craik, D. J., and G. C. Levy. 1984. Factors affecting accuracy in ^{13}C spin-lattice relaxation measurements. *Top. Carbon-13 NMR Spectros.* 4:241–275.

Doddrell, D., V. Glushko, and A. Allerhand. 1972. Theory of nuclear Overhauser enhancement and ^{13}C-^1H dipolar relaxation in proton-decoupled carbon-13 NMR spectra of macromolecules. *J. Chem. Phys.* 56:3683–3689.

Fuson, M. M., and J. H. Prestegard. 1983a. Dynamics of an interfacial methylene in dimyristoylphosphatidylcholine vesicles using carbon-13 spin relaxation. *Biochemistry.* 22:1311–1316.

Fuson, M. M., and J. H. Prestegard. 1983b. Dynamics of fatty acids in phospholipid vesicles using spin relaxation of proton-coupled carbon-13 spectra. *J. Am. Chem. Soc.* 105:168–176.

Gennis, R. B. 1989. Biomembranes: Molecular Structure and Function. Springer-Verlag, New York. 533 pp.

Grutzner, J. B., and R. E. Santini. 1975. Coherent broad-band decoupling—an alternative to proton noise decoupling in carbon-13 nuclear magnetic resonance spectroscopy. *J. Magn. Reson.* 19:173–187.

Huang, C. 1969. Studies on phosphatidylcholine vesicles. Formation and physical characteristics. *Biochemistry.* 8:344–351.

Huang, C., and J. T. Mason. 1978. Geometric packing constraints in egg phosphatidylcholine vesicles. *Proc. Natl. Acad. Sci. USA.* 75:308–310.

Karaborni, S., and J. P. O'Connell. 1990. Molecular dynamics simulations of model micelles. 4. Effects of chain length and head group characteristics. *J. Phys. Chem.* 94:2624–2631.

Kinosita, K., Jr., and A. Ikegami. 1984. Reevaluation of the wobbling dynamics of diphenylhexatriene in phosphatidylcholine and cholesterol/phosphatidylcholine membranes. *Biochim. Biophys. Acta.* 769: 523–527.

Kintanar, A., A. C. Kunwar, and E. Oldfield. 1986. Deuterium nuclear magnetic resonance spectroscopic study of the fluorescent probe diphenylhexatriene in model membrane systems. *Biochemistry.* 25: 6517–6524.

Korstanje, L. J., L. J. Van Faassen, and Y. K. Levine. 1989. Reorientational dynamics in lipid vesicles and liposomes studied with ESR: effects of hydration, curvature and unsaturation. *Biochim. Biophys. Acta.* 982:196–204.

Lafleur, M., P. R. Cullis, B. Fine, and M. Bloom. 1990. Comparison of the orientational order lipid chains in the Lα and HII phases. *Biochemistry.* 29:8325–8333.

Levitt, M. H., R. Freeman, and T. Frenkiel. 1982. Supercycles for broadband heteronuclear decoupling. *J. Magn. Reson.* 50:157–160.

Lipari, G., and A. Szabo. 1982. Model-free approach to the interpretation of nuclear magnetic resonance relaxation in macromolecules. 1. Theory and range of validity. *J. Am. Chem. Soc.* 104:4546–4559.

Lis, L. J., M. McAlister, N. Fuller, R. P. Rand, and V. A. Parsegian. 1982. Measurement of the lateral compressibility of several phospholipid bilayers. *Biophys. J.* 37:6677–6672.

Mayer, C., G. Grobner, K. Muller, K. Weisz, and G. Kothe. 1990. Orientation-dependent deuteron spin-lattice relaxation times in bilayer membranes: characterization of the overall lipid motion. *Chem. Phys. Lett.* 165:155–161.

Meier, P., E. Ohmes, and G. Kothe. 1986. Multipulse dynamic nuclear magnetic resonance of phospholipid membranes. *J. Chem. Phys.* 85:3598–3614.

Oldfield, E., M. Meadows, D. Rice, and R. Jacobs. 1978. Spectroscopic studies of specifically deuterium labelled membrane systems. Nuclear magnetic resonance investigation of the effects of cholesterol in model systems. *Biochemistry.* 17:2727–2739.

Parmar, Y. I., S. R. Wassall, and R. J. Cushley. 1984. Orientational order of phospholipid bilayers. ^{2}H NMR study of selectively deuterated palmitic acids in unilamellar vesicles. *J. Am. Chem. Soc.* 106:2434–2435.

Pastor, R. W., R. M. Venable, M. Karplus, and A. Szabo. 1988. A simulation based model of NMR T_1 relaxation in lipid bilayer vesicles. *J. Chem. Phys.* 89:1128–1140.

Peterson, N. O., and S. I. Chan. 1977. More on the motional state of lipid bilayer membranes: interpretation of order parameters obtained from nuclear magnetic resonance experiments. *Biochemistry.* 16:2657–2667.

Rajamoorthi, K., and M. F. Brown. 1991. Bilayers of arachidonic acid containing phospholipids studied by 2H and 31P NMR spectroscopy. *Biochemistry.* 30:4204–4212.

Rommel, E., F. Noack, P. Meier, and G. Kothe. 1988. Proton spin relaxation dispersion studies of phospholipid membranes. *J. Phys. Chem.* 97:2981–2987.

Seelig, J. 1977. Deuterium magnetic resonance: theory and application to lipid membranes. *Q. Rev. Biophys.* 10:353–418.

Seelig, J., and N. Waespe-Sarcevic. 1978. Molecular order in *cis* and *trans* unsaturated phospholipid bilayers. *Biochemistry.* 16:3310–3315.

Shaka, A. J., J. Keeler, and R. Freeman. 1983. Evaluation of a new broadband decoupling sequence: WALTZ-16. *J. Magn. Reson.* 53:313–340.

Soderman, O. 1986. The interaction constants in ^{13}C and ^{2}H nuclear magnetic resonance relaxation studies. *J. Magn. Reson.* 68:296–302.

Stockton, G. W., C. F. Polnaszek, A. P. Tulloch, F. Hasan, and I. C. P. Smith. 1976. Molecular motion and order in single-bilayer vesicles and multilamellar dispersions of egg lecithin and lecithin–cholesterol mixtures. A deuterium nuclear magnetic resonance study of specifically labelled lipids. *Biochemistry.* 15:954–966.

Stubbs, C. D., T. Kouyama, K. Kinosita, Jr., and A. Ikegami. 1981. Effect of double bonds on the dynamic properties of the hydrocarbon region of lecithin bilayers. *Biochemistry.* 20:4257–4262.

Taylor, M. G., T. Akiyama, H. Saito, and I. C. P. Smith. 1982. Direct observation of the properties of cholesterol in membranes by deuterium NMR. *Chem. Phys. Lipids.* 31:359–379.

Wade, C. G. 1985. Lateral diffusion of lipids. *In* Structural Properties of Cell Membranes: A Survey of Molecular Aspects of Membrane Structure and Function. G. Benga, editor. CRC Press, Boca Raton, FL. 51–76.